Limitations and Applications

The basic hypothesis of this paper is that the dispersion function (20) describes the propagation characteristics of any microstrip-like transmission line. So far, measurements on microstrip have supported this point of view.

A more general theoretical investigation than given in this paper would be necessary to explore the fundamental limitations on applying the dispersion function. Some points can be considered, however.

The dispersion relation applies only to the fundamental LSE mode. It probably holds closely only for thin ($b < \lambda/4$ in ϵ_s) substrates and strips that are not very wide ($w < \lambda/3$ in ϵ_s) to insure that the LSE mode is dominant, but these restrictions seldom arise in microstrip applications. Also, the dispersion relation takes on the correct value at infinite frequency, and so there is no clearly defined upper-frequency limit at which it no longer applies. The practical upper-frequency limit of microstrip, where every junction and discontinuity radiate strongly via surface wave modes [1], probably occurs before the dispersion function becomes unreliable.

Since the dispersion function appears to have general applicability to all structures having the same types of boundaries as microstrip and propagating an LSE mode, it would be expected to hold for microstrip with or without an enclosure, for the even and odd modes of the parallel-coupled microstrip, and possibly for other quasi-TEM structures, such as inhomogeneously loaded coaxial line. It would, of course, be necessary to have appropriate values for ϵ_s, ϵ_{e0}, Z_0, and G for each structure.

Acknowledgment

The author wishes to thank Dr. W. J. English for his technical discussions and T. J. Lynch for his careful measurements.

References

[1] C. Hartwig, D. Massé, and R. Pucel, "Frequency dependent behavior of microstrip," in *1968 G-MTT Symp. Dig.*, pp. 110–116.
[2] G. Zysman and D. Varon, "Wave propagation in microstrip transmission lines," in *1969 G-MTT Symp. Dig.*, pp. 3–9.
[3] O. Jain, V. Makios, and W. Chudobiak, "Coupled-mode model of dispersion in microstrip," *Electron. Lett.*, vol. 7, pp. 405–407, July 15, 1971.
[4] M. V. Schneider, "Microstrip dispersion," *Proc. IEEE (Special Issue on Computers in Design)* (Lett.), vol. 60, pp. 144–146, Jan. 1972.
[5] R. Collin, *Field Theory of Guided Waves*. New York: McGraw-Hill, 1960, p. 224.
[6] T. G. Bryant and J. A. Weiss, "MSTRIP (parameters of microstrip)," *IEEE Trans. Microwave Theory Tech.*, vol. MTT-19, pp. 418–419, Apr. 1971.
[7] C. Montgomery, R. Dicke, and E. Purcell, *Principles of Microwave Circuits* (M.I.T. Radiation Laboratory Series), vol. 8. New York: McGraw-Hill, 1948.
[8] P. Troughton, "Measurement techniques in microstrip," *Electron. Lett.*, vol. 5, pp. 25–26, Jan. 23, 1969.

Nonlinear Analysis of the Schottky-Barrier Mixer Diode

DOMINIC A. FLERI AND LEONARD D. COHEN

Abstract—**The waveshape of the local-oscillator voltage component that exists across the nonlinear junction of a Shottky-barrier diode is a fundamental determinant of mixer performance. This waveshape significantly differs from that of the total local-oscillator voltage impressed across the diode terminals since it is influenced by parasitics, particularly spreading resistance and contact inductance, which exist in series with the junction. The junction-voltage waveshapes resulting from a 9.375-GHz sinusoidal local-oscillator generator voltage are computed for three common equivalent-circuit models of the diode. In the first model the diode is represented by a nonlinear conductance in series with a fixed spreading resistance. The second model includes the nonlinear capacitance associated with the junction, and the third additionally includes the contact inductance. In each case, the junction-voltage waveshape is significantly nonsinusoidal. It is shown that the contact inductance can induce a peak inverse junction voltage that greatly exceeds the peak voltage impressed across the diode terminals. This parasitic reactance thus can have an important bearing on the burnout properties of the mixer diode.**

Manuscript received April 24, 1972; revised July 17, 1972.

D. A. Fleri was with the Bayside Research Center, General Telephone and Electronics Laboratories, Incorporated, Bayside, N. Y. 11360. He is now with the Department of Advanced Receiver Components and Subsystems, AIL, a division of Cutler-Hammer, Melville, N. Y.

L. D. Cohen is with the Bayside Research Center, General Telephone and Electronics Laboratories, Incorporated, Bayside, N. Y. 11360.

I. Introduction

OVER THE YEARS, a number of investigators [1]–[6] have published detailed mathematical treatments for determining the performance characteristics of semiconductor diode heterodyne mixers. These techniques basically involve the formulation of an admittance matrix or equivalent set of parameters, which describes the linearized small-signal current–voltage relations that exist among the coupled-signal, image, and intermediate frequency voltage components in the mixer. The admittance matrix facilitates the analytical determination of mixer conversion loss, as well as the associated RF and IF impedances. In general, the matrix elements are functions of both the amplitude and waveshape of the local-oscillator voltage component that exists across the nonlinear junction of the semiconductor diode. This waveshape was assumed to be sinusoidal by the early investigators because it was not practical to derive the exact waveshapes with the computational facilities then available. This assumption has been perpetuated over the years and is retained even in present-day analyses. As was pointed out by Barber [7], however, the actual waveshape of the local-oscillator junction voltage is significantly non-

TABLE I

NUMERICAL VALUES OF PARAMETERS USED IN COMPUTATIONS

Symbol	Definition	Value
R	Series Resistance	8.5 ohms*
C_0	Zero bias differential barrier capitance	0.08 pF*
L	Series contact inductance	1.7 nH*
ϕ	Barrier potential	0.9 volt**
I_s	Saturation current	10^{-13}A**
n	Quality factor related to Schottky barrier junction	1.1**
q	Electronic charge	1.6×10^{-19} coulomb
k	Boltzmann's constant	1.38×10^{-23} joules/°K
T	Absolute temperature	300°K
α	q ÷ (nkT)	34.8 volt^{-1}
$\omega/2\pi$	Local-oscillator frequency	9.375 GHz
Rg	Local oscillator internal resistance	50 ohms

* Measured at X-band.
** Measured at low frequency.

sinusoidal. Since the waveshape of the local-oscillator voltage component v_j is a fundamental determinant of mixer performance, the exact waveshape is computed here for three common equivalent circuit models of the diode. In the first model, the diode is represented simply by a nonlinear conductance $G(v_j)$ in series with spreading resistance R. The second model includes the nonlinear capacitance $C(v_j)$ associated with the junction, and the third model additionally includes the series contact inductance L. The values of the equivalent circuit parameters used in the computations are given in Table I. These correspond to actual experimental values derived from an unpackaged X-band GaAs Schottky-barrier diode [8]. R, L, and C_0 were determined from microwave measurements; the remaining parameters were obtained from low-frequency data.

II. ANALYSIS

In the first model, the effect of contact inductance and barrier capacitance is neglected; the Schottky-barrier diode is represented by a nonlinear conductance in series with a fixed resistance as shown in Fig. 1(a). The voltage $v_T(t)$ represents the local-oscillator generator voltage and is assumed to be sinusoidal. Since the junction conductance is nonlinear, $v_j(t)$ generally will be nonsinusoidal. The actual waveshape of $v_j(t)$ is governed by the equation

$$V_T \cos \omega t = (R_g + R)I_s[\exp(\alpha v_j) - 1] + v_j.$$

The Newton–Raphson [9] method was used to solve this equation numerically for $v_j(t)$; the results are given in Fig. 2 for several values of the parameter V_T. For V_T equal to or less than 0.5 V, v_j exhibits essentially the same waveshape as the sinusoidal generator voltage v_T. This results from the low level of current that flows through the junction at these levels of drive and the consequently negligible voltage drop developed across the 50-Ω generator resistance and the 8.5-Ω series resistance. For V_T equal or greater than 0.75 V, appreciable current flows through the junction during the positive half-cycle and the waveshape of v_j becomes significantly nonsinusoidal.

In the second model, the nonlinear differential barrier capacitance is included in the equivalent circuit model of the Schottky-barrier diode [Fig. 1(b)]. The barrier capacitance

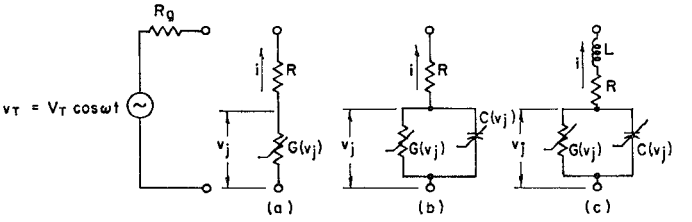

Fig. 1. Equivalent circuit of Schottky-barrier diode for (a) model I, (b) model II, and (c) model III.

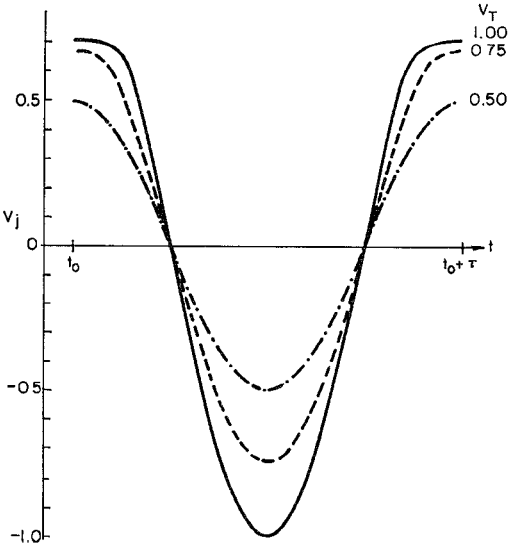

Fig. 2. Steady-state waveforms of local-oscillator voltage across nonlinear junction of model I for one complete RF cycle of period τ. At time t_0, $v_T = V_T$.

is a function of the local-oscillator junction voltage $v_j(t)$ and is represented by the expression

$$C(v_j) = \left.\frac{dQ}{dv}\right|_{v_j} = \frac{C_0}{[1 - v_j/\phi]^{1/2}}$$

where C_0 and ϕ are defined in Table I. The waveshape of $v_j(t)$ is derived from the voltage-loop equation which, as a consequence of (A-3), is a nonlinear first-order differential equation:

$$V_T \cos \omega t = v_j + (Rg + R) \cdot \left\{I_s[\exp(\alpha v_j) - 1] + C(v_j)\frac{dv_j}{dt}\right\}.$$

This equation was solved using a fourth-order Runge–Kutta numerical technique [10] subject to the condition that at $t = 0$, $v_j(0) = 0$. It was necessary to evolve v_j beyond the first several cycles to achieve the steady-state waveshape. Fig. 3 illustrates several steady-state waveshapes obtained for different values of the peak local-oscillator voltage V_T. In this particular case, the junction voltages closely approximate those computed for the resistive case, and therefore no essential difference in mixer performance should be expected.

At microwave frequencies the inductance associated with the electrical contact made to the junction has a predominant effect on the local-oscillator junction-voltage waveshape, and

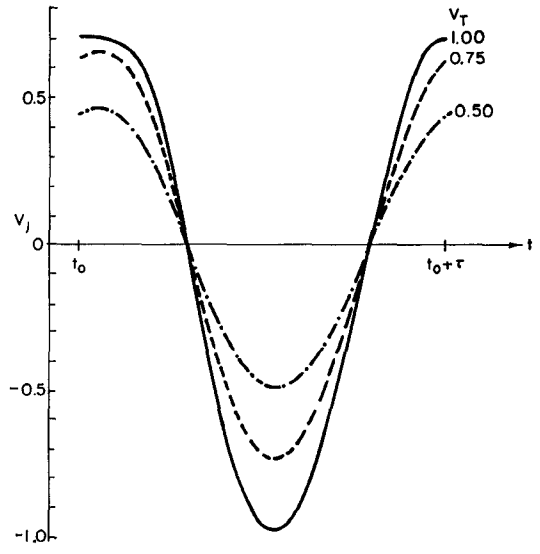

Fig. 3. Steady-state waveforms of local-oscillator voltage across nonlinear junction of model II for one complete RF cycle of period τ. At time t_0, $v_T = V_T$.

consequently it greatly influences mixer performance. In the third model, the Schottky-barrier diode is represented by the circuit model of Fig. 1(c), which includes the series contact inductance L. The local-oscillator junction voltage $v_j(t)$ is obtained by numerical solution of the coupled pair of nonlinear first-order differential equations that govern this equivalent circuit model:

$$V_T \cos \omega t = L\frac{di}{dt} + (Rg + R)i + v_j$$

$$i = I_s[\exp(\alpha v_j) - 1] + C(v_j)\frac{dv_j}{dt}.$$

The Runge–Kutta method [10] again was used to evolve the steady-state waveshape of $v_j(t)$, now subject to the conditions that at $t=0$, $i(0)=0$, and $v_j(0)=0$. Fig. 4 shows the waveshapes obtained using the experimental diode parameters of Table I and various values of the peak local-oscillator voltage. These waveshapes differ from those calculated in the previous cases in two essential respects: they remain positive for greater than a half-cycle and exhibit peak inverse voltages approximately two times the peak of the applied voltage V_T. The shape and time interval of the positive portion of $v_j(t)$ determine the shape and width of the conductance pulse, which in turn influences the conversion loss, impedance, and rectification properties of the mixer. The peak inverse voltage has a bearing on the noise and burnout properties of the diode. This analytical result correlates with the experimental observation that burnout is a voltage-related rather than power-related phenomenon [11] and indicates that the contact inductance may be a primary factor affecting mixer burnout.

III. Experimental

A. Simulation Experiments

It is evident that the contact inductance has a significant influence on the waveshape of the local-oscillator junction

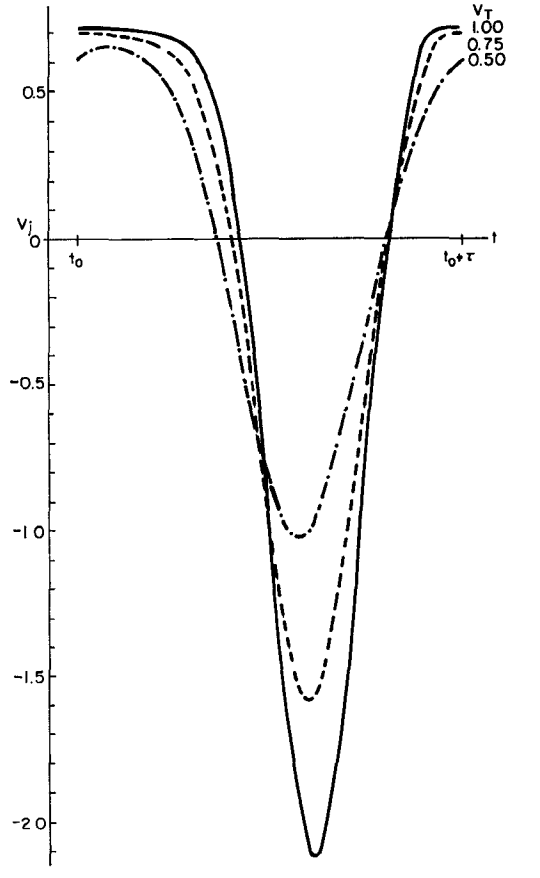

Fig. 4. Steady-state waveforms of local-oscillator voltage across nonlinear junction of model III for one complete RF cycle of period τ. At time t_0, $v_T = V_T$.

voltage. Fig. 5 shows a series of waveshapes computed for a range of inductance values extending from 0 to 2.5 nH and a zero-bias junction capacitance of 0.25 pF. In each case, the peak local-oscillator voltage was maintained at 1 V. As the inductance is increased from zero, the junction-voltage waveshape during the negative portion of the cycle changes from a sinusoid to a double-peaked characteristic of increasing amplitude. As the inductance is increased further, one peak increases while the other diminishes and the waveshape uniformly evolves into a narrow pulse of large amplitude. Further moderate increase in inductance does not change the basic shape of the junction-voltage waveform, but does influence the magnitude of the negative peak.

Since it is not feasible to observe the junction-voltage waveforms experimentally at 9.375 GHz, a low-frequency analog of the diode was constructed and its RF behavior was simulated in a manner similar to Barber [7]. The operating frequency was scaled to 0.9375 MHz to enable a direct observation of the simulated junction-voltage waveforms. Lumped elements were used to simulate the series resistance and contact inductance; a parallel combination of Schottky-barrier and Zener diodes was used to simulate a nonlinear junction conductance and capacitance. The impedance levels of the elements in the analog circuit approximated typical X-band values. Oscilloscope traces of the junction-voltage waveforms corresponding to various values of simulated contact inductance are shown in Fig. 6. In each photo, the

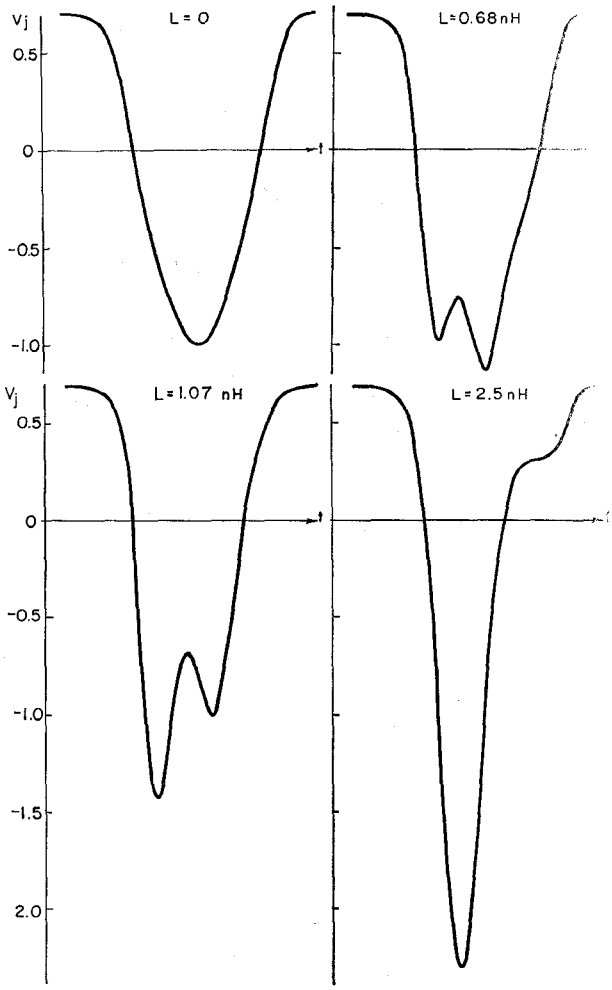

Fig. 5. Steady-state local-oscillator voltage across nonlinear junction of model III for $L=0$, 0.68 nH, 1.07 nH, and 2.5 nH.

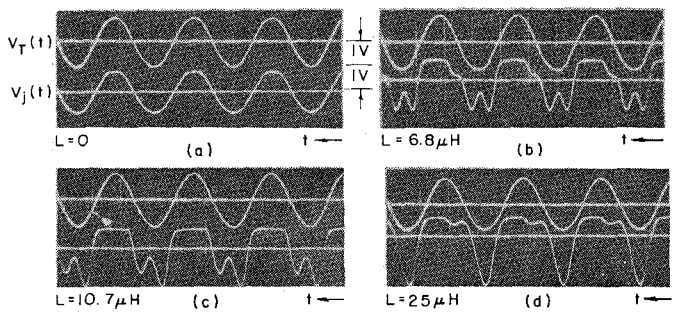

Fig. 6. Simulated steady-state junction voltages measured across nonlinear junction of low-frequency (0.9375 MHz) analog of model III for different values of simulated contact inductance. $R=8.5\ \Omega$ and simulated $C_0=250$ pF.

top trace represents the 0.9375-MHz voltage impressed across the diode terminals. The junction-voltage waveforms obtained in these simulation experiments closely resemble the computed waveforms depicted in Fig. 5 for corresponding values of inductance, and thus provide experimental corroboration of the analysis.

B. Rectification

The rectification characteristic of the Schottky-barrier diode provides a direct means of correlating the analytical

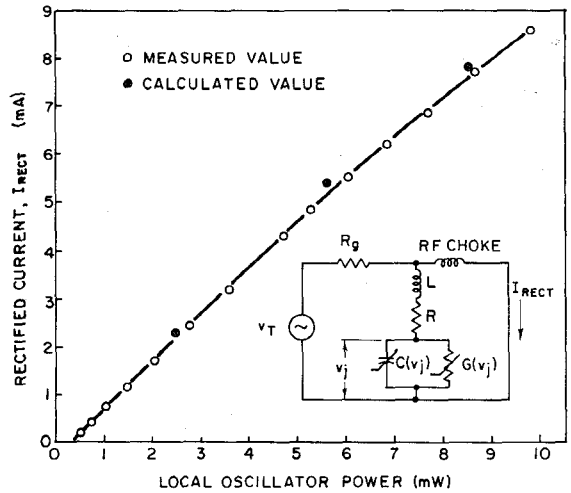

Fig. 7. Calculated and measured rectification characteristic of Schottky-barrier mixer diode for 9.375-GHz local-oscillator drive.

junction waveshapes with the actual microwave performance of the device. Fig. 7 shows rectified current versus local oscillator power obtained at 9.375 GHz with the Schottky-barrier diode represented in Table I. The diode was located in reduced height X-band rectangular waveguide of approximately 50 Ω. The solid points of Fig. 7 represent calculated values of rectified current. Each value was obtained by calculating the junction voltage v_j for a given level of available local oscillator power and then computing the dc component of the expression

$$I_s[\exp(\alpha v_j) - 1].$$

Rather close agreement exists between the measured characteristic and the calculated points. Each point falls somewhat above the experimental curve. This may be attributed in part to the zero dc return resistance assumed in the calculation (Fig. 7) in contrast to the 0.25 Ω, which actually existed in the experiment.

IV. Conclusion

Simulation experiments performed on the low-frequency analog of the unpackaged Schottky-barrier diode provided experimental validation of the analytical junction-voltage waveforms. Further validation is provided by the close agreement that exists between the calculated and measured microwave rectification characteristic of the diode. The series contact inductance has a critical effect on the local-oscillator junction-voltage waveshape, and consequently on the conversion loss and impedance levels of the mixer. Results were presented which demonstrate that the contact inductance can induce a peak inverse voltage that greatly exceeds the peak of the impressed generator voltage. The series inductance thus can also significantly affect the burnout properties of the diode.

Appendix

The current i_g through the nonlinear conductance and the charge Q on the nonlinear capacitance are functions of the total voltage v existing across the junction. This voltage consists of a large-amplitude local-oscillator component and small-amplitude signal, IF, and image components. The current and charge may each be represented by a Taylor-series

expansion about the local-oscillator voltage v_j:

$$i_g(v) = i_g(v_j) + \left.\frac{di_g}{dv}\right|_{v_j} (v - v_j) + \cdots \quad \text{(A-1a)}$$

$$Q(v) = Q(v_j) + \left.\frac{dQ}{dv}\right|_{v_j} (v - v_j) + \cdots \quad \text{(A-1b)}$$

where

$$\left.\frac{di_g}{dv}\right|_{v_j} \equiv G(v_j) = \text{differential junction conductance} \quad \text{(A-2a)}$$

$$\left.\frac{dQ}{dv}\right|_{v_j} \equiv C(v_j) = \text{differential junction capacitance.} \quad \text{(A-2b)}$$

The total current i through the junction due to the applied local-oscillator voltage is given by

$$i = i_g(v_j) + \dot{Q}(v_j)$$

where

$$i_g(v_j) = I_s[\exp(\alpha v_j) - 1]$$

and[1]

$$\dot{Q}(v_j) = C(v_j)\frac{dv_j}{dt}.$$

Thus

$$i = I_s[\exp(\alpha v_j) - 1] + C(v_j)\frac{dv_j}{dt}. \quad \text{(A-3)}$$

[1] Note that $\dot{Q}(v_j)$ does not equal $d/dt[C(v_j)v_j]$ since $C(v_j)$ is the differential capacitance. Thus $\dot{Q}(v_j) = (dQ(v_j)/dv_j)(dv_j/dt)$ where $(dQ(v_j)/dv_j) \equiv C(v_j)$. See [12].

ACKNOWLEDGMENT

The authors wish to thank Miss M. L. Hadley for invaluable assistance in computer programming, M. J. Urban for providing the GaAs Schottky-barrier diode, V. A. Lanzisera for performing the measurements, and Dr. B. A. Shortt for helpful advice and direction.

REFERENCES

[1] H. C. Torrey and C. A. Whitmer, *Crystal Rectifiers* (M.I.T. Radiation Laboratory Series), vol. 15. New York: McGraw-Hill, 1948.
[2] P. D. Strum, "Some aspects of mixer crystal performance," *Proc. IRE*, vol. 41, pp. 875–889, July 1953.
[3] G. C. Messenger and C. T. McCoy, "Theory and operation of crystal diodes as mixers," *Proc. IRE*, vol. 45, pp. 1269–1283, Sept. 1957.
[4] C. F. Edwards, "Frequency conversion by means of a nonlinear admittance," *Bell Syst. Tech. J.*, vol. 35, p. 1403, 1956.
[5] A. C. Macpherson, "An analysis of the diode mixer consisting of nonlinear capacitance and conductance and ohmic spreading resistance," *IRE Trans. Microwave Theory Tech.*, vol. MTT-5, pp. 43–51, Jan. 1957.
[6] C. A. Liechti, "Down-converters using Schottky-barrier diodes," *IEEE Trans. Electron Devices*, vol. ED-17, pp. 975–983, Nov. 1970.
[7] M. R. Barber, "Noise figure and conversion loss of the Schottky-barrier mixer diode," *IEEE Trans. Microwave Theory Tech.*, vol. MTT-15, pp. 629–635, Nov. 1967.
[8] L. D. Cohen, "Microwave characterization of the properties and performance of GaAs Schottky barrier mixer diodes," *Proc. IEEE (Special Issue on Satellite Communications)* (Lett.), vol. 59, pp. 288–289, Feb. 1971.
[9] G. A. Korn and T. M. Korn, *Mathematical Handbook for Scientists and Engineers*. New York: McGraw-Hill, 1968.
[10] M. Abromowitz and I. A. Stegun, *Handbook of Mathematical Functions* (Applied Mathematics Series 55). Washington, D. C.: NBS, 1967.
[11] Microwave Associates, Inc., "High rf burnout resistance mixer diodes," *Microwave J.*, vol. 13, p. 26, 1970.
[12] L. Blackwell and K. Kotzebue, *Semiconductor-Diode Parametric Amplifiers*. Englewood Cliffs, N. J.: Prentice-Hall, 1961, p. 107.

Design of Evanescent-Mode Waveguide Diplexers

C. K. MOK

***Abstract*—A novel design procedure for diplexers built in waveguides below cutoff is presented. The design permits the integral construction of a diplexer—the whole unit is built in a single waveguide, thereby dispensing with the T junction and connecting flanges —if coaxial termination is used at the common junction. The design utilizes foreshortened bandpass filters, and is valid for bandwidths of up to a few percent. Simple expressions on calculating the connecting lengths are arrived at. A satellite telemetry diplexer designed using the derived expressions yields results which are in agreement with computed values.**

Manuscript received May 1, 1972; revised July 21, 1972. This project was sponsored by the European Space Research Organisation.

The author is with the Standard Telecommunications Laboratories, an Associate of International Telephone and Telegraph, London Road, Harlow, Essex, England.

I. INTRODUCTION

DIPLEXERS in general take the form of two filters connected to a common port, and a fundamental problem in a diplexer is the matching of the two filters into this port. Various methods of diplexer design have been described in the past. Among these is the use of singly terminated low-pass and high-pass filters with Butterworth characteristics, which may be designed to be fully complementary [1], and hence may be connected together without the need of a correction network. This complementary nature is not present in Chebyshev singly terminated filters, and Veltrop and Wilds [2] have derived tables for quasi-complementary diplexers. Matthaei and Cristal [3] have described a design of partly